Supplementary Information for
Achieving accurate simulations of urban impacts on ozone at high resolution

J. Li[1*], M. Georgescu[1,2], P. Hyde[3], A. Mahalov[1], and M. Moustaoui[1]

[1] Julie Ann Wrigley Global Institute of Sustainability, School of Mathematical and Statistical Sciences, Arizona State University, Tempe, AZ 85287, USA

[2] School of Geographical Sciences and Urban Planning, Arizona State University, Tempe, AZ 85287, USA

[3] School for Engineering of Matter, Transport and Energy, Arizona State University, Tempe, AZ 85287, USA

Manuscript Submitted to Environmental Research Letters

This file includes:

1. WRF-chem and model setup
2. Anthropogenic emissions' downscaling and model simulation evaluation
3. Meteorological evaluation
4. Explanations of terms
5. References

[*]**Corresponding Author**: Jialun Li
Julie Ann Wrigley Global Institute of Sustainability
Arizona State University
Tempe, AZ 85287
Email: Jialun.Li@asu.edu

1. WRF-Chem and model setup

WRF-Chem is a two way coupled meteorology-chemistry model: Advanced Research weather WRF (WRF-ARW, Skamarock et al. 2008) and the chemical model (Chem)(Grell et al. 2005). WRF-ARW is a fully compressible, Euler nonhydrostatic, and multi-spatial scale model with multiple physical scheme selections. Details on WRF-ARW can be found in Skamarock et al (2008). The chemical model is dynamically coupled with ARW-WRF; explicit interactions between meteorology and chemistry are therefore considered. The chemical model also includes multiple selections of chemical reaction processes, emissions, photolysis schemes and other parameterization scheme selections. Details on WRF-Chem can be found in Grell et al (2005).

In this study, we pursue model simulations at high resolution. Considering the availability of meteorological forcing, we use four nested domains (see Figure S1) with the innermost domain resolution at 1-km to better represent topography and land surface features.

2. Anthropogenic emissions' downscaling and model simulation evaluation

In this study, the 4-km resolution U.S. Environmental Protection Agency (EPA) 2005 National Emissions Inventory (NEI05) data are used. This dataset covers the continuous U.S. and surrounding land areas (including northern Mexico and southern Canada). Since our inner most domain grid spacing is 1-km, downscaling NEI05 to 1-km resolution is necessary. WRF-Chem provides a scheme (which will be referred to as "Default" scheme hereafter) to re-map the NEI05 data to any resolution a WRF-Chem modeler desires. The Default method works well

when the model resolution is 4-km or coarser. When the WRF-Chem resolution is finer than 4-km, the Default method misrepresents emissions and the Default method generates abnormally high emissions values at some grid points.

Here, we present a new methodology to represent anthropogenic emissions at high-resolution for WRF-Chem simulations when the resolution of emissions are coarser than the model resolution. The monotonic cubic interpolation (MCI) method is used to downscale emissions from 4-km to 1-km resolution. Figure S2 shows the spatial distribution of "observed" (Fig. S2a) surface NOx in the Phoenix metro-area and in nearby areas at 12Z (early morning). Figure S2 additionally illustrates the downscaled NO_X distributions using the default (Figure S2b) and MCI (Figure S2c) methods. It is clear from Figure S2 that MCI produces results that are comparable to the 4-km NEI05 data. Furthermore, Figure S2 also shows that NOx emissions follow vehicular traffic, maintaining the highest emission rates from transportation corridors and the built environment.

Here, we first examine the performance of WRF-Chem ozone simulations initialized by anthropogenic emissions via the two downscaling methods (default and MCI). The model performance on meteorological fields will be discussed in next section. Figure S3 presents observed (Obs) versus simulated (Default and MCI labeled in the Figures) hourly ozone concentrations at different observation sites within the Phoenix metropolitan area and in surrounding rural areas from May 11, 2012 to May 14, 2012. Note that observations are based on hourly averages while the simulations reflect instantaneous values at the precise time of the hour. Figure S3 illustrates substantial improvements in simulated ozone concentration with WRF-Chem using the MCI method relative to the Default method for multiple stations.

Figure S4 is as Figure S3, but for a different event (June 09, 2011). In this case, although the simulated ozone concentrations with the Default method are generally acceptable in urban areas, the simulated results with the MCI method once again demonstrate substantial improvements. In addition, WRF-Chem with MCI produced better results than WRF-Chem with Default, in comparison with observation in the rural sites.

Note that effects of emissions from the two methods on ozone concentrations are not the same in magnitude based on results shown in Figures S3 and S4. Huang et al. (2013) have conducted sensitivity tests on how the changes of anthropogenic emissions affect ground-level ozone concentrations and their tests suggest that the relationships between anthropogenic emission changes and ozone concentrations are non-linear.

Model performance is also evaluated against EPA recommendations assessing simulated skill across a range of statistical metrics (EPA 1991; Table S1). EPA recommendations are based on the Mean Normalized Bias (MNB) and the Mean Normalized Gross Error (MNGE) for observation values of ozone mixing ratio greater than 40 ppb. These two metrics must have values that fall bellow ±15% (in magnitude) and 35% for MNB and MNGE, respectively, based on the U.S. EPA acceptance criteria for model performance. The values of MNB are -5.60% and -5.59% (underestimate within the required margin) for May 14, 2012 and June 09, 2011, respectively, for the cases where the anthropogenic emissions were initialized by MCI. The values of MNGE are 15.76 % and 15.70% for May 14, 2012 and June 09, 2011, respectively, also within the acceptance criteria recommended by USEPA. For the cases where the default interpolation is used, however, the values of MNB are -22% and -19% for the two episodes, falling outside of the EPA acceptable range for a skillful simulation. Although MNGE values

using the default downscaling method are within USEPA recommendation criteria (21% and 30% for each of the case study days), usage of the MCI downscaling method does indicate considerable improvement.

Table S1: Comparison of statistical variables with different anthropogenic emissions downscaling methods.

	MB (ppb)	RMSE (ppb)	NMB (%)	NME (%)	MNB (%)	MNGE (%)	IA	R	Status
06/09/11	-1.69	14.70	-6.32	15.32	-5.59	15.70	0.84	0.75	MCI
05/14/12	-1.50	14.75	-6.50	14.43	-5.60	15.76	0.81	0.74	MCI
06/09/11	-4.95	14.38	-19.15	21.43	-19.41	21.21	0.70	0.72	default
05/14/12	-7.91	20.90	-30.76	31.38	-22.10	29.98	0.51	0.60	default

MB: Mean Bias
RMSE: Root Mean Square Error
NMB: Normalized Mean Bias
NME: Normalized Mean Error
MNB: Mean Normalized Bias
MNGE: Mean Normalized Gross Error
IA: Index of Agreement
R: correlation coefficient

In Table S1, the Index of Agreement (IA) is defined:

$$IA = 1 - \left\{ \sum_{i}^{n} (P_i - O_i)^2 \Big/ \sum_{i}^{n} \left(|P_i - \overline{O}| - |O_i - \overline{O}| \right)^2 \right\}$$

Where, n is sample numbers, P represents model prediction and O represents observation.

The performance of WRF-Chem using the MCI method in capturing the spatiotemporal pattern of ozone variations was also analyzed. The IA and the correlation coefficient (R) between observations and simulations were calculated and compared with those obtained from the default method. Using MCI, the values of IA are 0.81 and 0.84 (the ideal value of IA would be 1) for May 14, 2012 and June 09, 2011, respectively. For the default method, these values are 0.5 and 0.70. The MCI method has larger values of IA compared to the default and therefore represents an improvement over the default method. The correlation coefficient (R) calculated for May 14 and Jun 09, 2011 of MCI and default are similar. Although MCI gives larger values of R, the differences between these values and those obtained from the default method are smaller compared to the other metrics (IA, MNB and MNGE). This indicates that both methods capture the phase and the timing of the diurnal cycle of ozone. Figure S3 and S4 show the comparison of the diurnal variation of ozone concentrations between observations and the model simulations using anthropogenic emissions obtained with the two disaggregation methods for the areas indicated in Fig. S2. The timing of the diurnal cycle is well captured using both methods, explaining the comparable values of the correlation coefficients

(Table S1). However, the amplitude of the diurnal cycle simulated by the MCI method is relatively closer to observations compared to the default method (Figs. S3 and S4).

We also use the two emissions-downscaling methods for the Los Angeles (LA) urban area for May 10-14, 2012 with similar model setup in domains 1, 2 and 3 while domains 4 for 1-km resolution covers LA and surrounding locales. Figure S5 presents the comparisons of the WRF-Chem simulations and observations for the LA region. The improvements are clear when MCI is used to downscale anthropogenic emissions to 1-km resolution from 4-km NEI05 data. Further details on this simulation will be reported separately.

The comparison presented in Figures S3, S4, and S5, and the statistical analysis presented in Table S1 demonstrates that the simulations using the newly developed method to downscale anthropogenic emissions achieve superior and more accurate results compared to those obtained from the default interpolation method. Therefore, the anthropogenic emissions for WRF-Chem simulations discussed in the text are from MCI for the innermost model domain.

3. Meteorological evaluation

We next discuss WRF-Chem performance on meteorological variables most relevant to photochemical reaction in the lower troposphere.

We use station data observed by Maricopa County Air Quality Department (MCAQD) and the Flood Control Department of Maricopa County (FCDMC) to evaluate WRF-Chem meteorological fields. The data from FCDMC can be downloaded online (http://alert.fcd.maricopa.gov/alert/Google/v3/gmap.html) while the data from MCAQD are provided by MCAQD staff. Both data sets include hourly data and are quality-controlled before

160 release (Daniel Henz and Ronald Pope, 2014, personal communications). In addition, the data
161 are also used to validate the 1.8-km resolution of WRF-ARW model performance for Arizona
162 State weather forecasts, which is operated by the University of Arizona (Daniel Henz, 2014,
163 personal communication). The data are first screened in order to remove those sites that
164 include too much missing data (more than 3 times per day). Then, the observation sites for
165 wind and temperature are categorized as four groups: sites in the desert, sites in the urban
166 areas, sites in rural near urban areas but not in urban, and sites in mountains. We evaluated the
167 urban areas. There are 8 sites available for 2-m air temperature and 7 sites available for wind
168 speed in the urban areas. No observations of short-wave (SW) radiation over urban areas were
169 found, and 17 sites for SW radiation from FCDMC in Domain 4 were used. In general, the WRF-
170 Chem model captures the basic features shown in the observations.

171 Figure S6 shows 10-m U-component wind (Urban run; V-component is very small) for
172 the case of May 14, 2012, and Case of June 09, 2011. Essentially, in Figure S6, the model
173 captured the diurnal cycle of the observed U-component. The model, however, overestimated
174 daytime wind speed in magnitude and the model also generated wind with 1-2 hours of time
175 shift during the wind direction transient periods between the model and the observed pattern,
176 which are common modeling phenomena as reported in previous studies (e.g., Lee and
177 Fernando, 2013, Lee et al. 2007). The wind statistical variables for the selected cases are listed
178 in Table S2. The sample numbers are over 600 for each case. Statistical results in Table S2
179 indicate that modeled winds for the Urban runs and the observed patterns exhibit linear
180 correlations with statistical significance ($P<0.01$).

181

Table S2: Wind statistics results between observations and simulations for the selected episodes in Urban run

	5/14/12		6/9/11	
	U10	V10	U10	V10
MB (m/s)	0.58	0.09	0.46	0.65
RMSE (m/s)	3.14	3.42	2.70	2.60
R	0.52	0.34	0.58	0.40
IA	0.71	0.64	0.70	0.64

Figure S7 shows the temperature diurnal cycles of the observation and the model with and without urban land cover. The model captured the daytime temperature very well for both Urban run and NO_urban run. During nighttime hours, the Urban runs captured the UHI intensity. With NO_urban run, the model could not have captured the observed temperature variability. The statistical variables are listed in Table S3 for Urban run.

Table S3: 2-m Temperature statistics results between observation and simulations for the selected episodes in Urban run

	5/14/12	6/9/11
MB (^{o}C)	-0.32	-0.34
RMSE (^{o}C)	2.47	2.08
R	0.92	0.94

Taha (2008) suggested using the criteria of temperature < ± 0.5 °C and wind speed <$\pm 0.5\ m/s$ to evaluate air pollution meteorological fields from model simulations in LA. As results presented in Table S2 and S3 indicate, the modeled meteorological variables generally satisfy these requirements.

The downward short-wave (SW) radiation between the observed and the model (Urban run) is also compared. The model captures the SW radiation diurnal cycle while overestimating the daytime radiation. Note that in the sunny and hot Phoenix metropolitan area, air temperature and radiation are sufficient for photochemical reactions. Emission availability and wind variation constrain ozone generation and distribution. During nighttime, air temperature can affect chemical reaction rates as well.

The above evaluation demonstrates that with the current model setup, the modeled meteorological fields captured the characteristics shown in the observations.

The averages of 2-m temperature differences (Urban run minus NO_urban run) for urban areas (shown in Figure 1) are plotted in Figure S8 for cases of May 14, 2012 and June 9, 2011. Figure S8 shows that temperature increases at night considerably, consistent with UHI observations and theory, and is only slightly offset by slight daytime cooling.

4. Explanations of terms

MM5: Pennsylvania University/National Center of Atmospheric Research Penn/MM5 Mesoscale model version 5 (MM5) (Grell et al. 1994): A limited-area, non-hydrostatic, terrain-following sigma-coordinate model designed to simulate or predict mesoscale atmospheric circulation. The model system includes pre-/postprocessing and physical model. The physical

model includes a series of atmospheric physical processes such as atmospheric boundary-layer physics, cloud microphysics, convective processes, radiation processes, and land surface processes. Each physical scheme has multiple choices.

RAMS: Regional Atmospheric Modeling System developed at Colorado State University (Pielke et al., 1992) is a mesoscale model system similar to MM5 in dynamical and physical representation. RAMS has relatively fewer physical scheme choices than MM5. RAMS can be used from global scale to the turbulence scale (such as large-Eddy simulations).

WRF: Weather Research and Forecast model system is the next generation of mesoscale modeling system (Skamarock et al. 2008). This model is governed by nonhydrostatic and fully compressible prognostic equations on a grid structure of the Arakawa-C type with multiple physical scheme choices. WRF can be used in operational mode (WRF-NMM) and for research purposes (WRF-ARW); it can be used for global applications to the turbulence scale (e.g., large-eddy simulations).

CMAQ: The Community Multiscale AIR Quality modeling system has been developed to represent multiple air quality issues (Byun and Schere, 2006).

MCI: Monotone Cubic Interpolation (MCI) is a variant of cubic interpolation that preserves monotonicity of the data set being interpolated (Fritsch and Carlson,1980).

NARR: North American Regional Reanalysis data (Mesiginer et al. 2006). The NARR model uses the very high resolution NCEP Eta Model (32km/45 layer) together with the Regional Data Assimilation System (RDAS) which, significantly, assimilates precipitation along with other variables. The improvements in the model/assimilation have resulted in a dataset with substantial improvements in the accuracy of temperature, winds and precipitation compared to

238 the NCEP-DOE Global Reanalysis 2. Currently, NARR has been output 8 times daily data at 29
239 pressure levels and most of the meteorological variables and the data are available since 1980.
240 MOZART-4: Modeled for Ozone and Related Chemical Tracers, Version 5, is an offline global
241 chemical transport model particularly suited for studies of the troposphere. The model
242 includes an expansion of the chemical mechanism to include more detailed hydrocarbon
243 chemistry and bulk aerosols. Online calculations of a number of processes, such as dry
244 deposition, emissions of isoprene and monoterpenes and photolysis frequencies, are now
245 included. Detail can be found in Emmons et al. (2010).
246 The GEOS-5 meteorology forecasts have been provided by the Global Modeling and
247 Assimilation Office (GMAO) at NASA Goddard Space Flight Center through the online data
248 portal in the NASA Center for Climate Simulation. The Goddard Earth Observing System Model,
249 Version 5 (GEOS-5) is a system of models integrated using the Earth System Modeling
250 Framework (ESMF). The GEOS-5 DAS (data assimilation system) integrates the GEOS-5 AGCM
251 with the Gridpoint Statistical Interpolation (GSI) atmospheric analysis developed jointly with
252 NOAA/NCEP/EMC. The GEOS-5 systems are being developed in the GMAO to support NASA's
253 earth science research in data analysis, observing system modeling and design, climate and
254 weather prediction, and basic research (https://gmao.gsfc.nasa.gov/systems/).
255 5. References
256 Byun D and Schene K, 2006 Review of the governing equations, computational algorithms, and
257 other components of the models 3: CMAQ modeling syst. *Appl. Mech. Rev*., **59**, 511-77
258 Emmons, L. et al, 2010 Description and evaluation of the Model for Ozone and Related chemical
259 Tracers, version 4 (MOZART-4), *Geosci. Model Dev*., **3**, 43-67, doi:10.5194/gmd-3-43-2010

EPA, 1991 Guideline for Regulatory Application of the Urban Airshed Model, US EPAReport No. EPA-450/4-91-013, Office of Air Quality Planning and Standards, Technical Support Division, Research Triangle Park, North Carolina, USA.

Fast J, Doran J and Shaw W 2000 The evolution of the boundary layer and its effect on air chemistry in the Phoenix area *J. Geophys. Res*. **105(D18)** 22833-22848

Fritsch F., and Carlson R., 1980 Monotone Piecewise Cubic Interpolation". *SIAM Journal on Numerical Analysis* (*SIAM)* **17 (2)** 238–246.doi:10.1137/0717021

Grell, G., Dudhia J., and Stauffer D, 1994: A description of the Fifth-Generation Penn State?NCAR Mesoscale Model (MM5). NCAR/Penn-398+STR (www.mmm.ucar.edu/mm5/documents/mm5-desc-doc.html)

Grell G A, Peckham S E , Schmitz R , McKeen S A , Frost G , Skamarock W C , and Eder B 2005 Fully coupled "online" chemistry within the WRF model *Atmos. Environ.* **39** 6957–6975 doi:10.1016/j.atmosenv.2005.04.027

Huang M, et al, 2013 Impact of Southern California anthropogenic emissions on ozone pollution in the mountain states: Model analysis and observational evidence from *space J. Geophys. Res-Atmos*. **118**, 12784-12803

Lee S and Fernando H 2013 Dispersion of an urban photochemical plume in Phoenix metropolitan area *Atmos. Environ*. **80** 152-160

Lee S, Fernando H, Princevac M, Zajic D, Sinesf M, Mcculley J and Anderson J 2003 Transport and diffusion of ozone in the nocturnal and morning planetary boundary layer of the Phoenix Valley *Environ. Fluid Mech.* **3** 331-362

Lee S , H. Fernando H and Grossman-Clarke S 2007 MM5-SMOKE-CMAQ as a modeling tool for 8-h ozone regulatory enforcement: application to the state of Arizona *Environ. Model. Assess.* **12** 63-74

Ryu Y, Baik J, Kwak K, Kim S and Moon N 2013 Impact of urban land-surface forcing on ozone air quality in the Seoul metropolitan area *Atmos. Chemi. Phys*. **13** 2177-2194

Skamarock W, Klemp J, Dudhia J, Gill D, Barker D, Wang W and Powers J 2008 A description the Advanced Research WRF version 3, www.mmm.ucar.edu/wrf/users/docs/arw_v3.pdf

Taha H. 2008 Urban surface modification as a potential ozone air-quality improvement strategy in California: A meoscale modeling study *Bound.-Layer Meteorol*. **127** 219-239

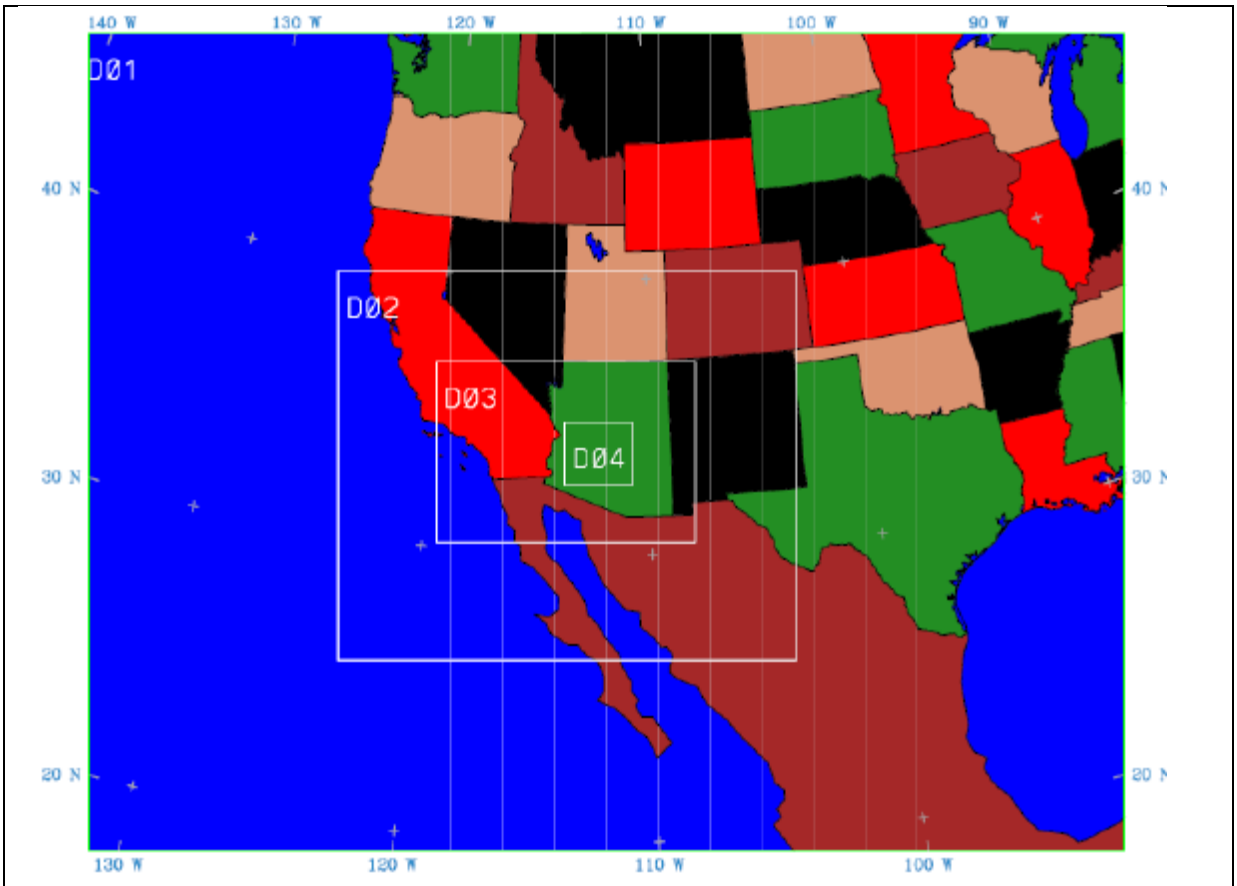

Figure S1: Model domains D01 represents Domain-1 with 36-km of resolution. D02 represents domain-2 with 12-km of resolution. D03 represents Domain-3 with 4-km resolution and D04 represents domain-4 with 1-km resolution.

307

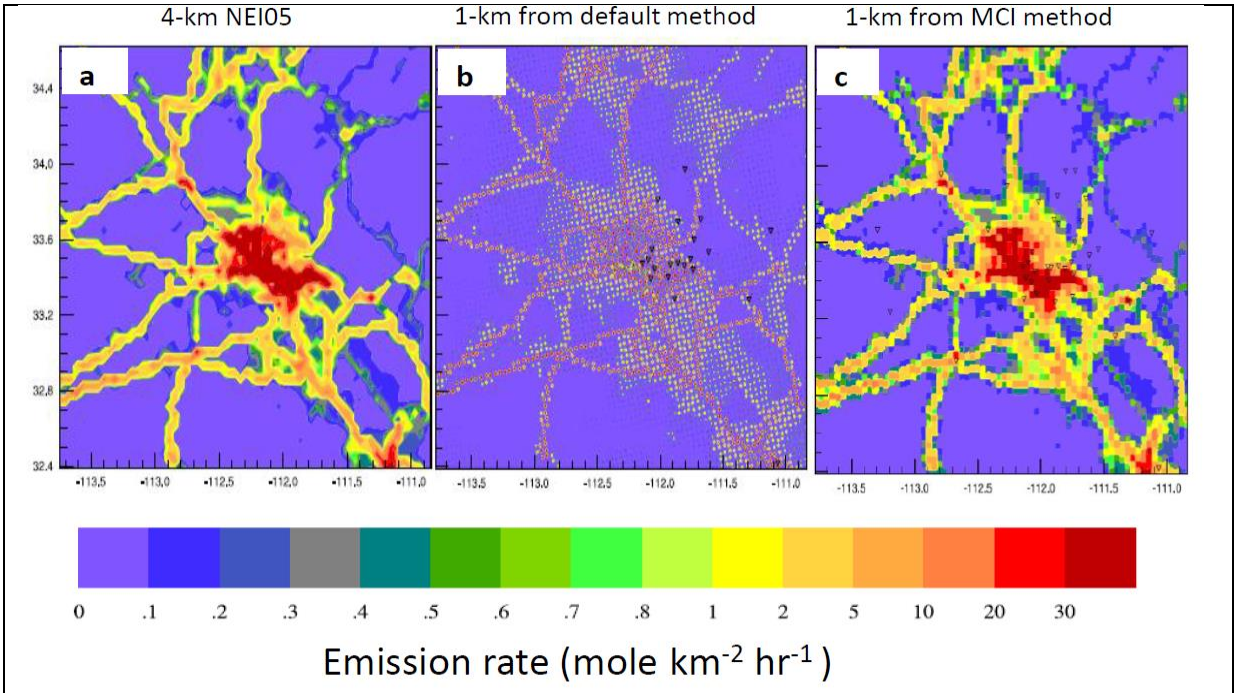

Figure S2: Spatial distribution of anthropogenic emissions (NOx here) in Phoenix and surrounding areas at 12Z from (a) 4-km resolution EPA 2005 Emissions Inventory (NEI05); (b) downscaling to 1-km resolution using the default method provided with the WRF-Chem system; and (c) downscaling to 1-km resolution using the Monotonic Cubic Interpolation (MCI) method.

308

309

310

311

312

313

314

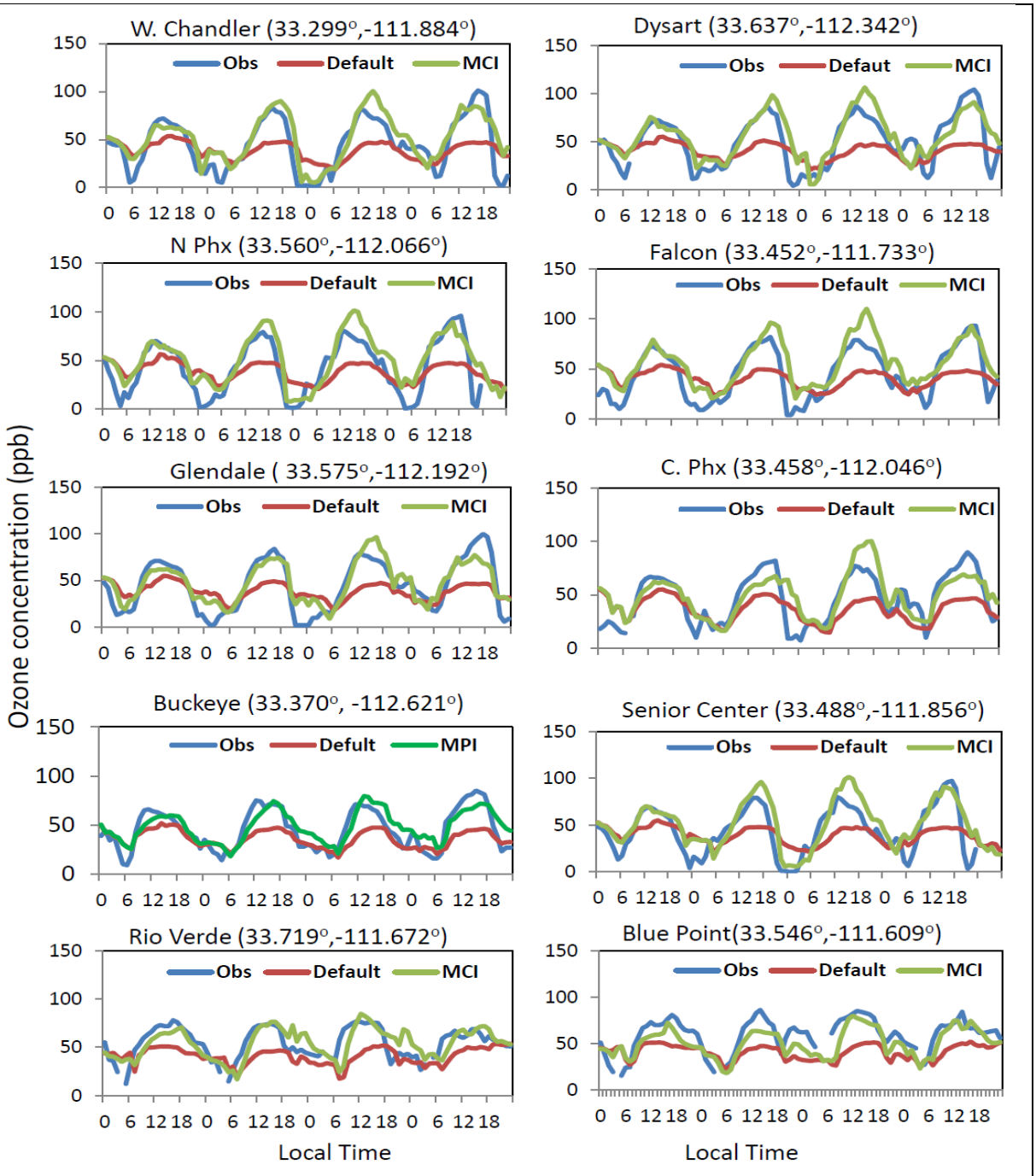

Figure S3: Ozone concentration comparisons between Observations (Obs) and WRF-Chem output when different methods are used to downscale anthropogenic emissions (AEs). Obs mean observations at different sites for the period from May 11 to May 15, 2012. Default represents WRF-Chem output when the AEs are downscaled by the Default method and MCI represents WRF-Chem output when AEs are downscaled by the MCI method. Ozone exceedance was observed on May 14 at the locations N. Phx, Glendale, W. Chandler, Dysart, C. Phx and Senior Center. The dates in the figure cover the period from May 11 to May 15, 2012.

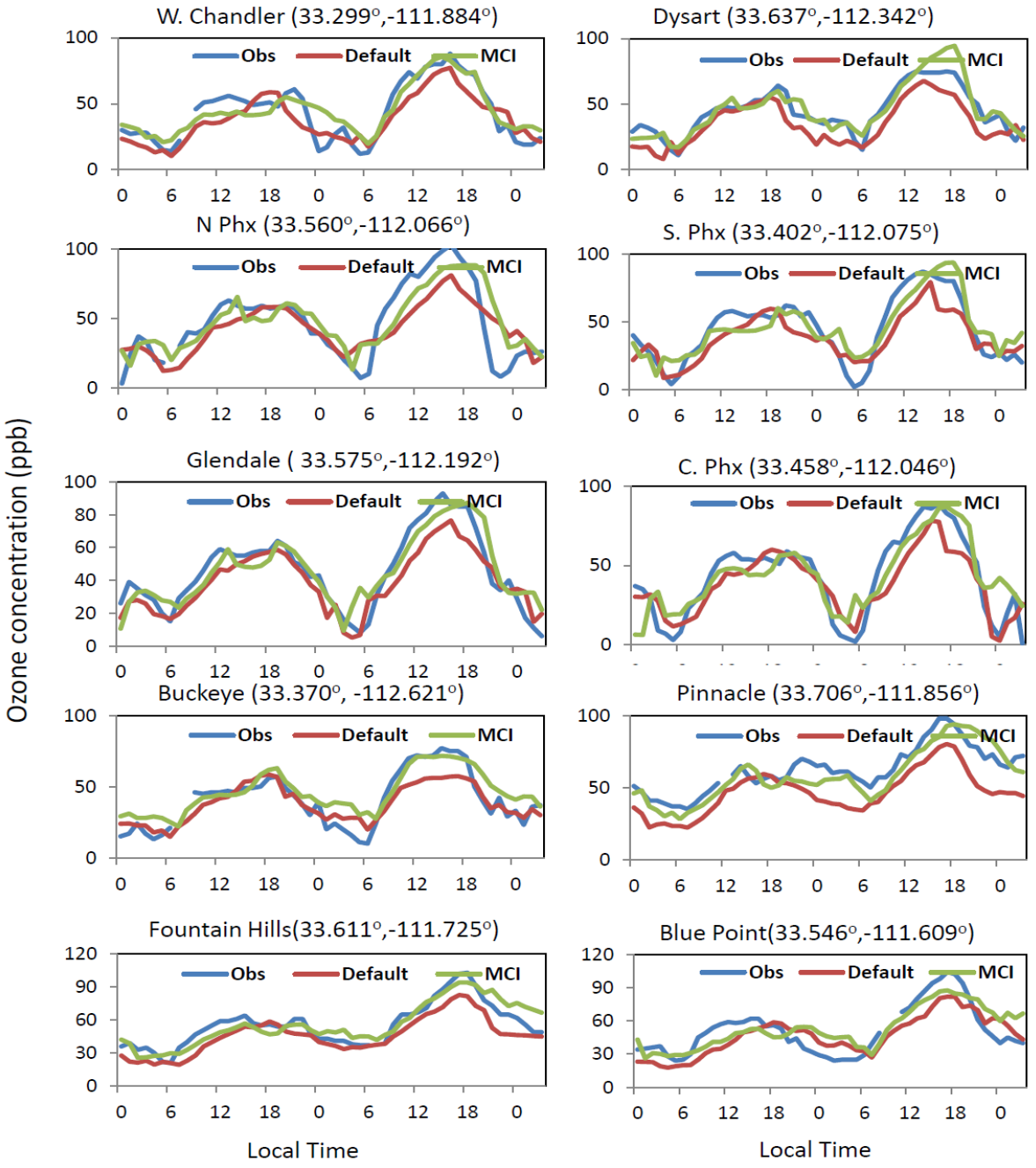

Figure S4: Ozone concentration comparisons between Observations (Obs) and WRF-Chem output when different methods are used to downscale anthropogenic emissions (AEs). Obs represents observations at different sites for the period from June 08 to June 10, 2011. Default represents WRF-Chem output when the AEs are downscaled by the Default method and MCI represents WRF-Chem output when AEs are downscaled by the MCI method. Ozone exceedance was observed on June 09 at the locations N. Phx, Glendale, C. Phx, Pinnacle, Fountain Hills and Blue Point. The dates in the figure covers the period from June 8 to June 9, 2011.

315

316

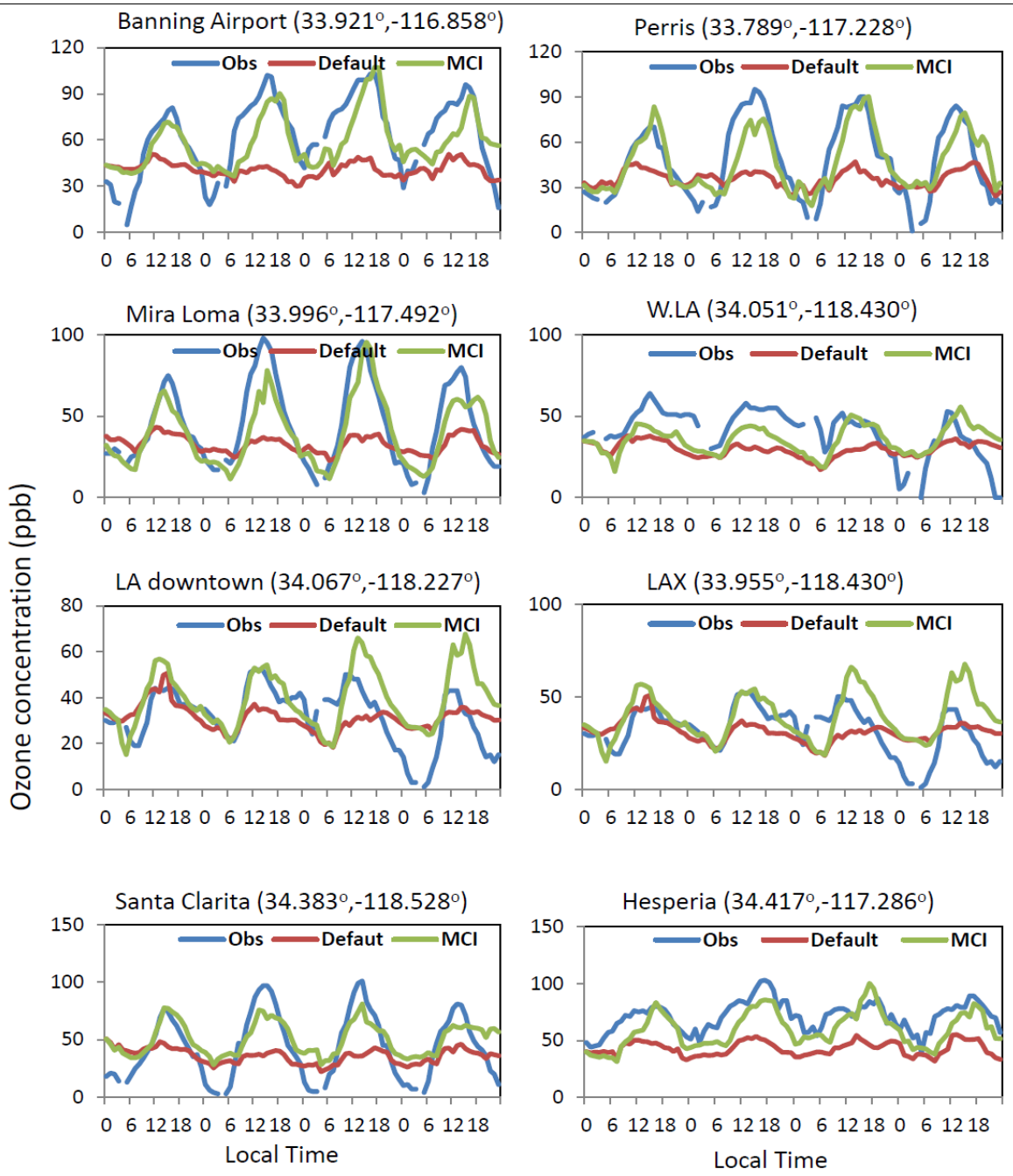

Figure S5: Ozone concentration comparisons between Observations (Obs) and WRF-Chem output when different methods are used to downscale anthropogenic emissions (AEs). Default represents WRF-Chem output when the AEs are downscaled by the Default method and MCI represents WRF-Chem output when AEs are downscaled by the MCI method. The dates in the figure cover the period from May 11 to May 15, 2012.

317

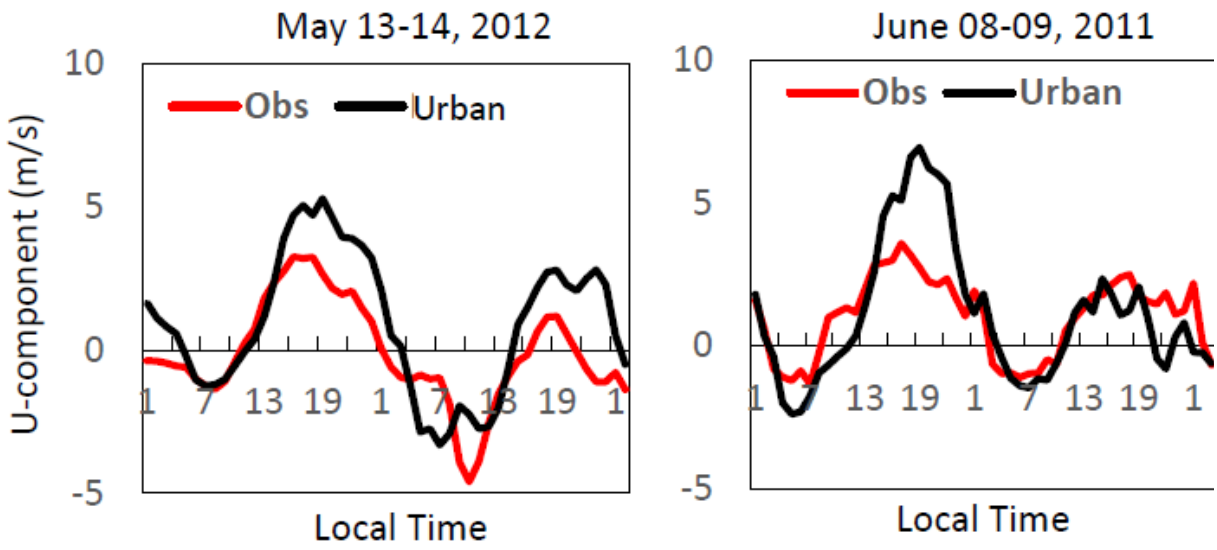

Figure S6: Averaged wind speed (U-component) comparisons between observation and model (with Urban runs) closest to the observation site for different episodes. V-component is very small in the two cases and not plotted.

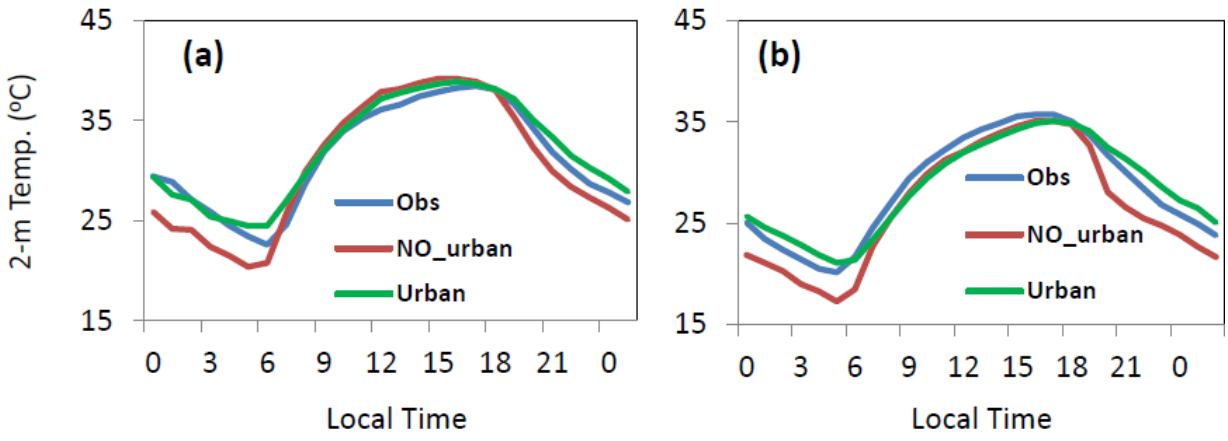

Figure S7: Air temperature at 2-m comparisons between observations and models with/without urban land cover runs for different episodes. (a) May 14, 2012, (b) June 09, 2011.

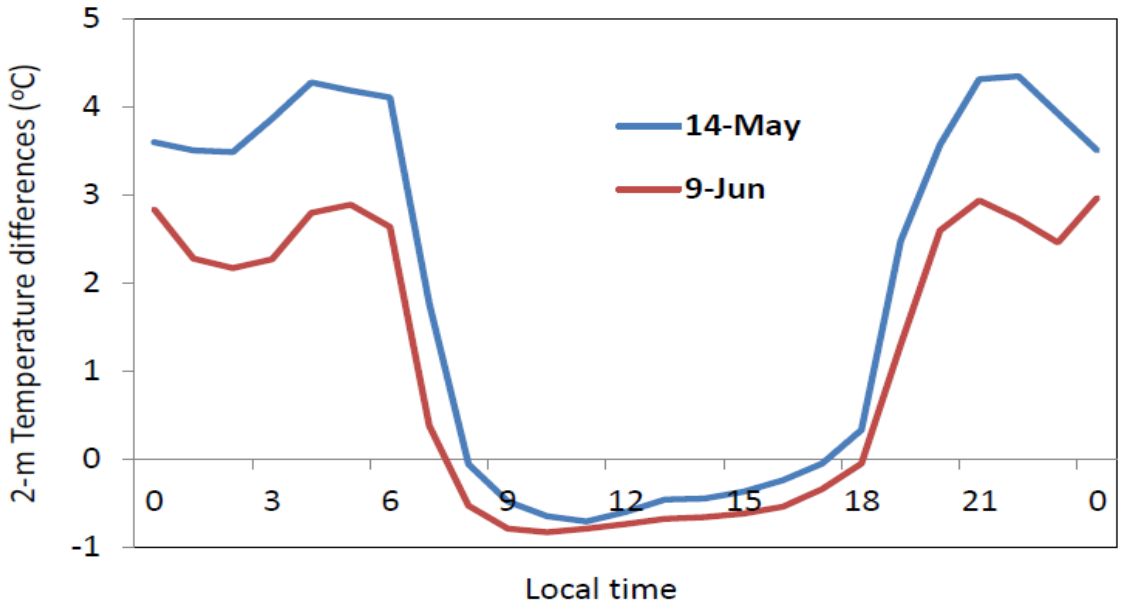

Figure S8: Time series of averaged 2-m temperature differences (Urban run minus NO_urban run) in the urban area (area shown in Figure 1) for the two episodes.